AIP Applied Physics Letters

Graphene-silver nanowire hybrid structure as a transparent and current spreading electrode in ultraviolet light emitting diodes

Tae Hoon Seo, Bo Kyoung Kim, GangU Shin, Changhyup Lee, Myung Jong Kim, Hyunsoo Kim, and Eun-Kyung Suh

Citation: Applied Physics Letters **103**, 051105 (2013); doi: 10.1063/1.4817256
View online: http://dx.doi.org/10.1063/1.4817256
View Table of Contents: http://scitation.aip.org/content/aip/journal/apl/103/5?ver=pdfcov
Published by the AIP Publishing

Graphene-silver nanowire hybrid structure as a transparent and current spreading electrode in ultraviolet light emitting diodes

Tae Hoon Seo,[1] Bo Kyoung Kim,[1] GangU Shin,[1] Changhyup Lee,[2] Myung Jong Kim,[2] Hyunsoo Kim,[1] and Eun-Kyung Suh[1,a)]
[1]*School of Semiconductor and Chemical Engineering, Semiconductor Physics Research Center, Chonbuk National University, Jeonju 561-756, South Korea*
[2]*Soft Innovative Materials Research Center, Korea Institute of Science and Technology, Jeonbuk 565-905, South Korea*

(Received 18 June 2013; accepted 12 July 2013; published online 30 July 2013)

We report a device that combines graphene film and Ag nanowires (AgNWs) as transparent and current spreading electrodes for ultra-violet (UV) light emitting diode (LED) with interesting characteristics for the potential use in the deep UV region. The current-voltage characteristics and electroluminescence (EL) performance show that graphene network on AgNWs well-operates as a transparent and current spreading electrode in UV LED devices. In addition, scanning electron microscopy and EL images exhibit that graphene film act as the protection layer of AgNWs layer as well as a transparent conducting network, by bridging AgNWs. © *2013 AIP Publishing LLC*. [http://dx.doi.org/10.1063/1.4817256]

GaN-based light emitting diodes (LEDs) in the visible and ultraviolet (UV) wavelength regions have been studied intensively for applications such as full color or white LED displays, indoor or outdoor LED lighting, and backlights for liquid-crystal display.[1–3] In particular, UV-LED can be used in germicidal instrumentation, biological agent identification, chemical sensing, fluorescence excitation, and optical data storage. However, the reported external quantum efficiency of the UV-LEDs is still limited by several factors including high threading dislocation, high resistivity of *p*-GaN due to Mg doping difficulty, high optical absorption in the *p*-GaN clad/contact layers, etc.[4,5] In particular, typical *p*-type cap or *p*-AlGaN top layer with high lateral sheet resistance and low carrier mobility due to high activation energy resulted in severe current crowding under the vertical direction of the electrode, incomplete current spreading through the full emitting area, and poor device reliability. For these reasons, transparent conductive films have been widely used as a transparent and current spreading electrode (TCSE) in UV LEDs. The most commonly used materials in the case of visible wavelength LEDs are doped metal oxides, particularly indium tin oxide (ITO) owing to its good physical properties of high optical transmittance and low sheet resistance. Unfortunately, it appears that ITO layer has several drawbacks such as soaring prices due to indium scarcity, brittleness, sensitivity to acidic and base chemical sources, and high processing temperature.[6,7] Furthermore, ITO shows high absorption in UV region, making it difficult for practical use as a TCSE in UV LEDs. Hence, an alternative transparent electrode is required with superb optical transmittance especially at UV wavelength range and good electrical performances similar to or better than those of ITO layer.

Recently, several materials, such as graphene, Ag nanowires (AgNW) film, and carbon nanotube film, have emerged as promising next-generation TCSE of UV LEDs due to their high mechanical flexibility as well as good optical transparency and electrical conductivity.[8–10] Even though graphene has a high mobility and excellent optical transmittance especially in the UV wavelength region, the adoption of bare graphene on *p*-GaN for TCSE of UV LED gives rise to problems such as a large turn on voltage, low hole injection efficiency toward active region, severe current crowding under a *p*-metal electrode, and heat generation because of its high sheet resistance.[11,12]

To this end, AgNW films have attracted significant attention because of their advantages in materials properties such as low sheet resistance and high optical transmittance at UV wavelength region. Furthermore, the mesh-like geometry of AgNW causes surface texturing effect and an enhanced plasmonic resonance effect, which can efficiently increase light extraction efficiency. However, disadvantages of AgNWs film, such as a long-term stability issue, typical high nanowire-nanowire junction resistance, and the poor adhesion to substrate, have limited application as a TCSE material in UV-LED device. In particular, when AgNWs film is exposed to air at ambient conditions, AgNWs can be easily oxidized, leading to sharp increase of sheet resistance and mutation of properties,[13] which makes it difficult for practical use.

To resolve problems with high sheet resistance of graphene and long-term stability of the AgNWs film, in this work, a prototype current spreading electrode for UV-LED with UV emission at a wavelength of 375 nm was constructed by combining one-dimensional AgNWs and two-dimensional graphene layer, and compared the performance with each of AgNWs film and graphene layer, respectively. AgNWs film on the *p*-GaN layer act as the lateral current transport pathway because of its low sheet resistance, and graphene film, known to be chemically inert up to around

a)Author to whom correspondence should be addressed. E-mail: eksuh@jbnu.ac.kr. Tel.: +82-63-270-3606.

500 °C in general, act as the protection layer to a pure and unoxidized AgNWs film as well as an ultra-thin transparent conducting network, connecting AgNWs.

The AlInGaN-based UV-LEDs were grown on sapphire substrate by metal-organic chemical vapor deposition. A 25 nm-thick GaN buffer layer was deposited on sapphire substrate at 550 °C before the growth of a 1.5 μm thick un-doped GaN layer and a Si doped *n*-GaN layer with a thickness of 2.0 μm at 1040 °C. Then, five pairs of $In_{0.03}Ga_{0.97}N$ QWs and $Al_{0.08}Ga_{0.92}N$ barrier layers with thicknesses of 2 and 12 nm, respectively, were grown at 800 °C. Finally, 25 nm-thick Mg-doped *p*-$Al_{0.25}Ga_{0.75}N$ electron blocking layer and 100 nm-thick *p*-GaN contact layer were grown at 1040 °C. Rapid thermal annealing (RTA) was performed at 940 °C for 40 s under N_2 ambient to activate Mg dopants.

We fabricated three types of discrete UV-LED with a chip size of $350 \times 350\ \mu m^2$, each having different TCSEs: AgNWs, bare graphene, and graphene on AgNWs. The patterned region was covered with a protective photoresist (PR) as an etchant mask to make mesa region. Mesa region was defined by an inductively coupled plasma etcher using Cl_2/BCl_3 gases until *n*-GaN layer was exposed for *n*-electrode ohmic contact. Prior to graphene transfer, the TCSE area was selectively opened using a PR lift-off process. Then, AgNWs film was spin coated at a speed of 1000 rpm onto the *p*-GaN surface of LED wafer using spin coater. Large scale graphene layers were synthesized on ~25 μm thick Cu-foil by chemical vapor deposition (CVD) method. Details can be found in Ref. 14. After the removal of the PR mask, CVD-grown graphene films with poly methyl methacrylate (PMMA) were transferred onto the UV-LED pre-patterned with AgNWs film. Thereafter, the PMMA was removed using hot acetone. Then, graphene films were patterned by an inductively coupled plasma (ICP)-reactive ion etcher using O_2 plasma. Finally, Cr (50 nm)/Au (250 nm) metals for the *p*- as well as the *n*-electrodes were deposited onto both the graphene on AgNWs film and the n-GaN layer using electron beam evaporator. For comparison, UV LEDs with bare graphene and with AgNWs were fabricated using conventional LED-fabrication step. A schematic diagram of fabricated UV-LED with graphene network on AgNWs as a TCSE is shown in Fig. 1.

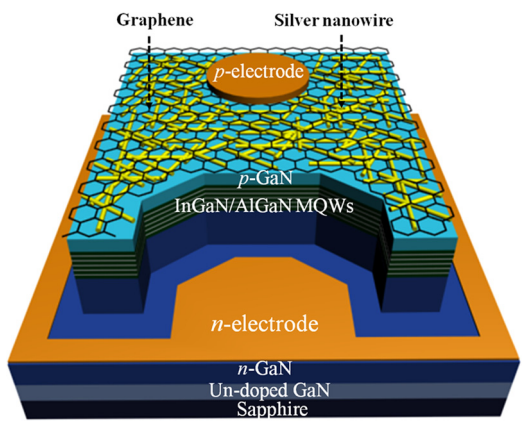

FIG. 1. Schematic diagram of fabricated InGaN/AlGaN MQWs UV LED with Ag nanowire-graphene hybrid structure as the transparent and current spreading electrode.

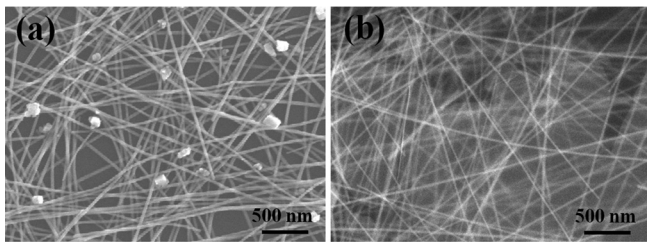

FIG. 2. SEM images of (a) pristine AgNWs, and (b) graphene-AgNWs hybrid structure after 1 day of exposure.

Figures 2(a) and 2(b) show scanning electron microscopy (SEM) images of AgNWs and graphene network on AgNWs. The average length and diameter of AgNWs are about 5–20 μm and 15 nm, respectively. AgNWs form a conducting network, which is essential for carrier transport as shown in Figs. 2(a) and 2(b). In Fig. 2(a), silver oxides were clearly observed on the AgNWs surface, indicating that these oxides are the major origin of increased contact resistance between AgNWs.[15] However, SEM image of AgNWs covered by graphene network does not contain silver oxides around AgNWs because gas and moisture cannot permeate the graphene layer. It means that stability and impermeability properties of graphene prevent the oxidation of AgNWs under various conditions.[16]

Figure 3(a) shows the Ag 3d core-level spectra of AgNWs and graphene-AgNWs hybrid structure. The Ag 3d peak of AgNWs was observed into two doublets corresponding to $3d_{3/2}$ and $3d_{5/2}$ binding energies at 367.7 and 373.4 eV, respectively. After transferring graphene on AgNWs, the Ag $3d_{3/2}$ peak has shifted about 0.6 eV from 367.7 eV of pristine AgNWs to 368.3 eV of graphene network on AgNWs. The upshift in Ag 3*d* peak position is a proof of charge transfer from AgNWs to the localized sp^2 domains of the graphene film.[17]

The 2D-to-G band intensity ratio and peak position of the G band in the Raman spectra are sensitive to the charge doping between AgNWs and graphene due to the charge transfer driven by the difference in the workfunction.[17] The Raman spectra of bare graphene film and graphene network on AgNWs on 300 nm SiO_2/Si substrate excited with a 514 nm-line of an Ar ion laser are shown in Fig. 3(b). Two prominent peaks in the Raman spectra of bare and AgNWs-graphene films were observed: A G-band associated with phonons of the doubly degenerated zone center E_{2g} mode at the Γ point and a 2D band involving two phonons with opposite momentum in the highest optical branch near the K point of the Brillouin zone.[18] Raman spectra show a feature similar to that of monolayer graphene, i.e., 2D-to-G intensity ratio greater than 1 and symmetric 2D band with a full width at half maximum of 35 cm^{-1}. For the case of graphene network on AgNWs, the decrease of 2D/G intensity ratio, and the upshift of the G peak were observed due to the charge doping effect associated with the direct charge transfer between AgNWs and graphene.[19] Moreover, the D band located at around 1360 cm^{-1}, which is related with levels of defects, local disordered carbon, wrinkles or edges in graphene film, is slightly increased. The increased D band in the graphene film on AgNWs indicates the formation of disorders or defects caused by the AgNWs incorporated in the graphene film.[20]

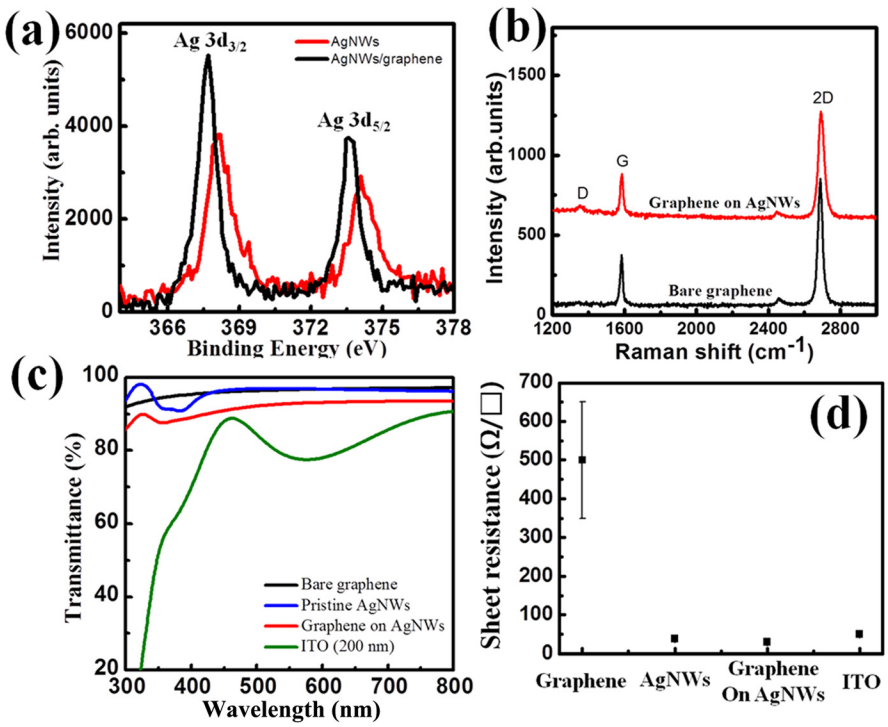

FIG. 3. (a) XPS Ag 3d core-level spectra of pristine AgNWs and graphene-AgNWs hybrid structure, respectively, (b) Raman spectra of bare graphene and graphene on AgNWs, respectively, (c) transmittance characteristics and (d) sheet resistance of bare graphene film, pristine AgNWs, and graphene network on AgNWs, respectively.

The optical transmittance and sheet resistance are important when the top electrode film is used as the TCSE in LEDs because the efficiency of LEDs is strongly dependent on the transmittance and sheet resistance of TCSE. The optical transmittance of graphene network on AgNWs was compared to those of bare graphene and AgNWs, respectively, on a polished sapphire substrate. As shown in Fig. 3(c), the transmittance of bare graphene film, AgNWs, and the combination of graphene on AgNWs were found to be 93, 90.2, and 86.3%, respectively, at the wavelength of 375 nm. The AgNWs show relatively strong absorption around 390 nm wavelength region due to localized surface plasmons of AgNW.[21] In the case of graphene network on AgNWs, the plasmon absorption of AgNWs was reduced because graphene film, which connects between AgNWs and covers the thin AgNWs, suppresses the collective oscillation of the free electron through AgNWs induced by an interacting electromagnetic field.[21,22]

To confirm the change in electrical conductivity after combining AgNWs and graphene, the Hall measurement was carried out; the sheet resistance was 30 ± 3 Ω/□ for the graphene network on AgNWs which is much lower than the value of 500 ± 100 Ω/□ and 50 ± 5 Ω/□ of bare graphene and AgNWs as can be seen in Fig. 3(d). The obtained low sheet resistance are due to the increased carrier density by charge transfer as well as the opening up new conduction channels by bridging grain boundaries and line disruption in graphene film.[23,24]

Figure 4(a) shows I–V characteristics for fabricated UV-LEDs with bare graphene, AgNWs, and graphene network on AgNWs, respectively. All UV-LEDs present rectifying behavior without showing a reverse bias leakage current. In Fig. 4(a), the forward voltage (V_f) at an input current of 20 mA were found to be 10.9, 6.7, and 4.48 V for LEDs with TCSEs of graphene film, AgNWs, graphene network on AgNWs, respectively. The V_f value for UV LED with graphene network on AgNWs decreased dramatically compared to those of LEDs with graphene film or with AgNWs owing to the reduced sheet resistance and the effective current spreading. This result shows that graphene network on AgNWs can provide efficient current diffusion pathways and are able to provide injected current to the active junctions of LED through *p*-GaN layer. Details of the carrier transportation, ohmic characteristics, and conductivity of contact interface between graphene film and AgNWs are under study. The electroluminescence (EL) spectra of InGaN/AlGaN MQWs UV-LEDs with various TCSEs at an injection current of 20 mA are shown in Fig. 4(b). Even though the transmittance of graphene on AgNWs at the wavelength of 375 nm was lower than those of AgNWs or graphene film, the EL intensity of UV-LED with graphene network on AgNWs was significantly enhanced compared to those of other electrodes because of effective current spreading and injection efficiency toward *p*-GaN surface caused by the low sheet and contact resistance of the graphene on AgNWs electrode; the increase of the conductivity through additional current spreading paths and surface texturing effect by AgNWs result in the strong EL. The main point of using graphene on AgNWs was observed in EL images of Fig. 4(c). The emission power of UV LED with bare graphene layer was non-uniform and only bright near the *p*-electrode area due to the high sheet resistance of graphene. Also, the light emission was not uniform in the device with AgNWs showing strong light emission only near the *p*-electrode due to incomplete current spreading by the formation of AgNWs with sparse and non-uniform networks. In the case of graphene network on AgNWs, a bright and uniform light emission was observed over the whole surface of UV LED. The UV LED with graphene network on AgNWs does not show any joule heating or oxidation up to injection current of 100 mA investigated in this work and operates without any degradation under continuous current

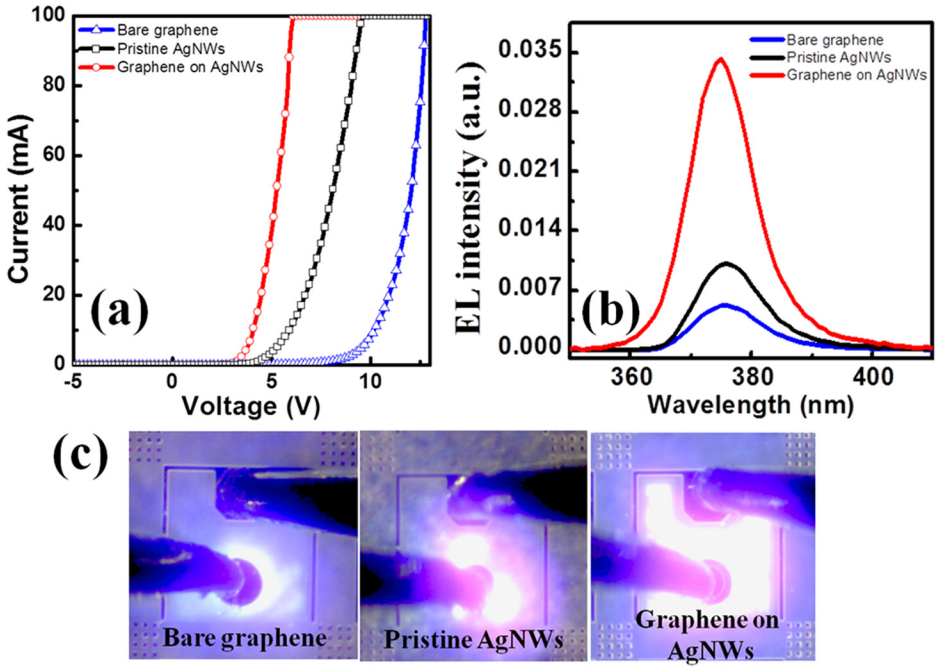

FIG. 4. (a) The I-V characteristics, (b) EL spectra, and (c) EL images at an injection current of 20 mA in InGaN/AlGaN MQW UV-LEDs with various TCSEs.:Bare graphene film, Pristine AgNWs, and graphene on AgNWs.

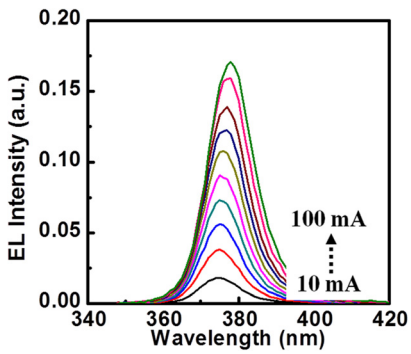

FIG. 5. EL spectra as a function of current in the UV LED with graphene network on AgNWs.

injection up to 300 s. These results show that graphene film as TCSE act as an ultra-thin transparent conducting network, connecting AgNWs.

Figure 5 shows the EL spectra of UV LED with graphene network on AgNWs as a function of injection current from 10 to 100 mA. Note that the EL spectrum was not observed from LEDs with graphene film or AgNWs only when the injection current exceeds 20 mA because the device failed by an extreme amount of power accumulation under the *p*-electrode. As can be seen in Fig. 5, our UV LEDs with graphene network on AgNWs operate well at injection currents up to 100 mA examined. The EL emission wavelength only slightly red-shifted from 375 nm at 10 mA to 378 nm at 100 mA. The emission spectrum of strained InGaN QW under increasing injection current is determined by competition between spectral redshift mechanism of piezoelectricity-induced quantum-confined stark effect and blueshift mechanism of filling of indium induced band tail state.[25] In UV LEDs, band filling effect should be weak for insignificant indium induced quantum dot-like states in MQWs, resulting in the red-shift of the EL peak with increasing injection current.

In conclusion, we propose graphene film on AgNWs as a transparent and current spreading electrode in InGaN/AlGaN MQW UV-LEDs, which demonstrated significant enhancement of I–V and EL characteristics at 375 nm light emission. The advantage of using graphene film on AgNWs as a TCSE is expected to be important in deep UV-LEDs because of the rapid decrease of optical transmittance of conventional metal oxide material TCSE such as ITO in the deep UV region.

This work was supported by Basic Science Research Program through the National Research Foundation of Korea (NRF) funded by the Ministry of Education, Science and Technology (2010-0019694 and 2012R1A1A3011103)

[1]F. A. Ponce and D. P. Bour, Nature **386**, 351 (1997).
[2]E. F. Schubert and J. K. Kim, Science **308**, 1274 (2005).
[3]M. R. Krames, O. B. Shchekin, R. Mueller-Mach, G. O. Mueller, L. Zhou, G. Harbers, and M. G. Craford, J. Disp. Technol. **3**, 160 (2007).
[4]W. Wu, C. Elsass, A. Abare, M. Mack, S. Keller, P. Petroff, S. Denbaars, J. Speck, and S. Rosner, Appl. Phys. Lett. **72**, 692 (1998).
[5]D. Cherns, S. Henley, and F. Ponce, Appl. Phys. Lett. **78**, 2691 (2001).
[6]Z. Chen, B. Cotterell, W. Wang, E. Guenther, and S. Chua, Thin Solid Films **394**, 201 (2001).
[7]T. Minami, Thin Solid Films **516**, 5822 (2008).
[8]D. S. Hecht, L. Hu, and G. Irvin, Adv. Mater. **23**, 1482 (2011).
[9]L. Hu, H. S. Kim, J.-Y. Lee, P. Peumans, and Y. Cui, ACS Nano **4**, 2955 (2010).
[10]T. H. Seo, K. J. Lee, T. S. Oh, Y. S. Lee, H. Jeong, A. H. Park, H. Kim, Y. R. Choi, E.-K. Suh, T. V. Cuong, V. H. Pham, J. S. Chung, and E. J. Kim, Appl. Phys. Lett. **98**, 251114 (2011).
[11]B.-J. Kim, C. Lee, Y. Jung, K. H. Baik, M. A. Mastro, J. K. Hite, C. R. Eddy, Jr., and J. Kim, Appl. Phys. Lett. **99**, 143101 (2011).
[12]J.-P. Shim, T. H. Seo, J.-H. Min, C. M. Kang, E.-K. Suh, and D.-S. Lee, Appl. Phys. Lett. **102**, 151115 (2013).
[13]C. H. Liu and X. Yu, Nanoscale Res. Lett. **6**, 75 (2011).
[14]H. Cho, C. Lee, I. S. Oh, S. Park, H. C. Kim, and M. J. Kim, Carbon Lett. **13**, 205 (2012).
[15]J. L. Elechiguerra, L. Larios-Lopez, C. Liu, D. Garcia-Gutierrez, A. Camacho-Bragado, and M. J. Yacaman, Chem. Mater. **17**, 6042 (2005).
[16]S. Chen, L. Brown, M. Levendorf, W. Cai, S.-Y. Ju, J. Edgeworth, X. Li, C. W. Magnuson, A. Velamakanni, R. D. Piner, J. Kang, J. Park, and R. S. Ruoff, ACS Nano **5**, 1321 (2011).
[17]Z. Deng, M. Chen, and L. Wu, J. Phys. Chem. C **111**, 11692 (2007).
[18]A. C. Ferrari, Solid State Commun. **143**, 47 (2007).

[19]K. S. Subrahmanyam, A. K. Manna, S. K. Pati, and C. N. R. Rao, Chem. Phys. Lett. **497**, 70 (2010).
[20]J. M. Lee, J. W. Choung, J. Yi, D. H. Lee, M. Samal, D. K. Yi, C.-H. Lee, G.-C. Yi, U. Paik, J. A. Rogers, and W. I. Park, Nano Lett. **10**, 2783 (2010).
[21]Y. Sun, B. Gates, B. Mayers, and Y. Xia, Nano Lett. **2**, 165 (2002).
[22]L. Yang, G. H. Li, and L. D. Zhang, Appl. Phys. Lett. **76**, 1537 (2000).
[23]I. N. Kholmanov, C. W. Magnuson, A. E. Aliev, H. Li, B. Zhang, J. W. Suk, L. L. Zhang, E. Peng, S. H. Mousavi, A. B. Khanikaev, R. Piner, G. Shvets, and R. S. Ruoff, Nano Lett. **12**, 5679 (2012).
[24]C. Jeong, P. Nair, M. Khan, M. Lundstrom, and M. A. Alam, Nano Lett. **11**, 5020 (2011).
[25]E. Kuokstis, J. W. Yang, G. Simin, M. A. Khan, R. Gaska, and M. S. Shur, Appl. Phys. Lett. **80**, 977 (2002).